

Using Piper trilinear diagrams and principal component analysis to determine variation in hydrochemical facies and understand the evolution of groundwater in Sidi Slimane Region, Morocco

Nabil Darwesh^{1*}, Mona Allam^{2,3}, Qingyan Meng^{2*}, Al Aizari Helfdhallah¹,
Naser Ramzy S. M⁴, Khadija El Kharrim¹, Ali A. Al Maliki⁵ and Driss Belghyti¹

1- Laboratory of Agro-physiology, Biotechnology, Environment and Quality, Faculty of Sciences, Ibn Tofail University, Kenitra, Morocco.

2-Aerospace Information Research Institute, Chinese Academy of Sciences, Beijing 100094, China.

3-Environment & Climate Change Research Institute, National Water Research Center, Egypt.

4- General Directorate of Environmental Health, Sana'a, Yemen

5- Ministry of Science and Technology, Environment and Water Directorate, Al Jadryia, Baghdad, Iraq

*Corresponding authors: Nabil Darwesh aboali3000@gmail.com; Qingyan Meng mengqy@radi.ac.cn

ARTICLE INFO

Article History:

Received: Oct. 17, 2019

Accepted: Nov. 26, 2019

Online: Nov.30, 2019

Keywords:

Groundwater quality
Piper trilinear diagram
Sidi Slimane
Correlation matrix
Morocco

ABSTRACT

The water quality of groundwater is one of the most important issues for development and life societies. The chemical parameters of the groundwater play a significant role in classifying and assessing water quality. In this study, twenty samples were collected from different locations in a rural region to determine the hydrochemical facies characteristics and understand the evolution of groundwater quality in the Sidi Slimane area in Morocco. Piper trilinear diagram and principal component analysis (PCA) were used to find out the major contributing parameters involved in groundwater samples. The results showed that the analytical values obtained when plotted on Piper's plots revealed that the alkalis (Sodium, Potassium), are significantly dominant over alkaline earth metals (Calcium, Magnesium) and the strong acidic anions (Chlorides, Sulfates) dominant over the weak acidic anions (Carbonates and Bicarbonates). Piper trilinear diagram classified 90 % of the samples from the study area under $\text{Na}^+ - \text{K}^+ - \text{Cl}^- - \text{SO}_4^{2-}$ type and only 10 % samples under $\text{Ca}^{2+} - \text{Mg}^{2+} - \text{Cl}^- - \text{SO}_4^{2-}$ type. The Piper plots highlighted that the groundwater is dominant of Na-Cl type and the water types originating from halite dissolution (saline) in the study area. Also, correlation matrix showed that 95%, 100%, 65%, 75%, 65% and 55% of the examined groundwaters exhibit higher concentration of Sodium, Ammonium, Calcium, Electrical Conductivity EC, Chloride, and Nitrate respectively than the maximum acceptable limit of the Moroccan's standards for drinking water. PCA suggests a significant mutual positive correlation between two main groups of parameters (EC, Ca^{2+} , Mg^{2+} , K^+ , Na^+ , HCO_3^- and Cl^-) and (pH, NH_4^+ , SO_4^{2-} , and NO_3^-). The output of PCA analysis is in confirmation with that of the Piper trilinear diagram and the correlation matrix to identify the characteristics of the samples and aid to comprehend their spatial distribution.

INTRODUCTION

Groundwater is the main source of drinking water in many parts of the world. Groundwater is subject to pollution due to several trace elements and ions that occur naturally or as the result of human activities at critical concentrations. The quality of the groundwater has to be evaluated to avoid or, at least, to minimize negative impacts on human health (WHO, 2011). As Morocco's water resources are limited, Groundwater is exposed to agricultural, industrial, or urban pollution (Belghiti *et al.*,

2013). Renewable water resources are estimated at 29 billion m³ per year, approximately 1044 m³ per capita/year in 1998. By 2020, it's estimated to be 786 m³ per capita/year (Bzioui, 2004). The water resources in the coastal region of the Gharb are threatened by the pollution caused due to a growing industry in cities and increasing urbanization. Indeed, global growth in the economy, population density, and infrastructure developments increased stress on the available water and on its quality also. (Aremu *et al.*, 2017). The present work aims to evaluate the quality of groundwater and understand the hydrochemical facies characteristics at Sidi Slimane area in Morocco, using a Piper trilinear diagram. Further, statistical methods such as principal component analysis (PCA) was used to detect the major contributing parameters in the groundwater samples (Ravikumar and Somashekar, 2017).

Study area

The City of Sidi Slimane is a small city in the northwestern center of Morocco in the Rabat-Salé-Kénitra economic region, is located between the major cities of Kenitra and Meknes (Fig. 1). The city recorded a population of 92,989, According to the 2014 General Population and Housing Moroccan census (MONOGRAPHIE GENERALE, 2015). The study area locates between 34°13'N and 5°42'W 34° 13' 0" N, 5° 42' 0" W (34.216667, -5.7), WGS84 (Callegarin *et al.*, 2011; Mehanned *et al.*, 2014).

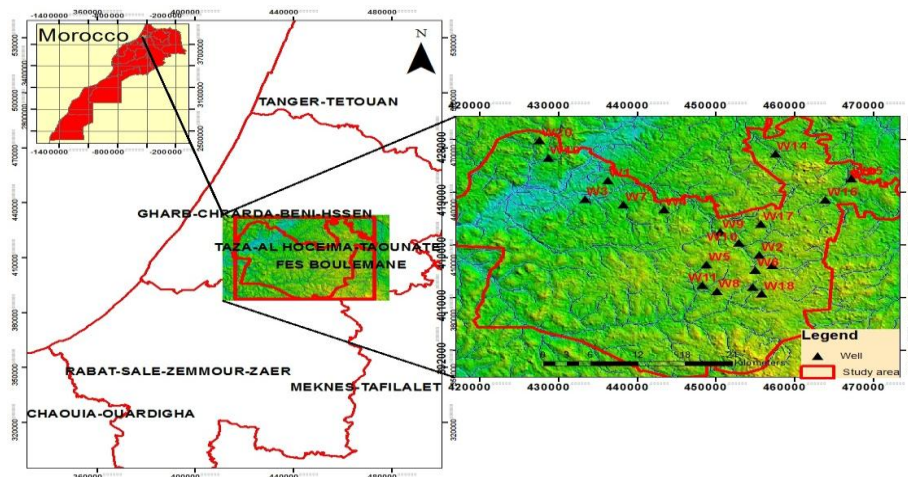


Fig. 1: Map of the study area showing sampling locations

It covers an area of 4000 km². It is characterized by a semi-arid climate with high humidity of the air. The annual rainfall is 445 mm on average, the wettest month is December with an average of 77mm. The dry period is relatively long and starts from May to September. During this period, the monthly rainfall does not exceed 5 mm. The average temperature varies between 10 C° in January and 26 C° in July and August. However, the average maximum temperature is 40 °C in July, while the average minimum is 1 °C in December. (Callegarin *et al.*, 2011; Mehanned *et al.*, 2014). It is also of varying surfaces with varying degrees of elevation from sea level 12 m.

METHOD AND MATERIAL

Twenty groundwater samples were collected in May 2015 from Sidi Slimane region at Morocco. The samples were collected after pumping for 10 min. Clean and dry polyethylene bottles were used for samples collection, following the standard

procedures. The samples were transported at 4°C in portable coolers to the Lab, where the chemical analysis was performed. Collecting, transporting and analyzing of samples were performed according to the standard recommended analytical methods (APHA, 2005 ; Rodier *et al.*, 2009). The pH was measured using a pH meter (WTW Inolab). The Electrical Conductivity (EC) was measured using a conductmeter (Thermo ORION 3 STAR). Calcium (Ca^{2+}) and Magnesium (Mg^{2+}) were determined using complex meter EDTA. Sodium (Na^+) and Potassium (K^+) were determined by a flame photometer (JENWAY PFP7). Carbonates (CO_3^{--}) and the Bicarbonates (HCO_3^-) were analyzed by a solution of sulfuric acid 0.02 N in the presence of phenolphthalein and bromocresol indicator green colored. Chlorides (Cl^-) were determined by silver nitrate in the presence of potassium chromate solution. Sulfates (SO_4^{2-}) was examined by spectrophotometer (V-1100). Determination of Nitrate NO_3^- and ammoniums NH_4^+ by distillation by (VELP SCIENTIFICA UOK148) distillation apparatus. in the presence of a catalyst respectively oxide of magnesium and alloy of DEVA GDR. NH_4^+ and NO_3^- were collected in a solution of boric acid and Calibrate eventually by H_2SO_4 . Piper trilinear diagrams were plotted using Aquachem 3.7 software package. Further, the analytical results shown in Table 1 were used as input for the principal component (PCA) analysis. Statistical analysis was carried out using statistical package for social sciences (xlstat2018) Excel. The global Mapper program was used in the preparation of a topographic map of the study area.

RESULTS AND DISCUSSION

The quality of groundwater in Sidi Slimane Region was evaluated according to Moroccan standards for drinking water. The the average analysis of physicochemical analysis is summarized in (Table 1).

Hydroge Ion concentration (pH)

The pH of water refer to its acidity or alkalinity to by detection the concentration of the hydrogen ions present in the water. The value of pH is an indicator of the quality of water WHO (2011) The measured values of pH were recorded between 6.7 and 7.9 with an average 7.3 ± 0.28 (Table 1). The pH values are valid according to the Moroccan Standards for drinking water, for all tested samples (Fig. 2).

Table1: Statistic of physico-chemical analyses of groundwater for 20 samples

Parameter	Min	Max	Average	StDev	Morocco standerd of drink water
EC	1540	17550	4915	3772	<2700
pH	6.74	7.85	7.3165	0.28	6.5-9.5
Ca^{2+}	56.8	290	167.5	70.5	<100
Mg^{2+}	26.64	192.24	71.13	42.58	<100
Na^+	186	1959	738	507	<200
K^+	2.34	11.7	5.946	2.742	12
Cl^-	265	2929	1111	776	<750
SO_4^{2-}	13.7	223.4	79	58	<250
HCO_3^-	145.2	799.1	461.6	158.5	500
NO_3^-	14.3	386.9	99.5	96.6	<50
NH_4^+	0.9	7.02	2.125	1.302	<0.5

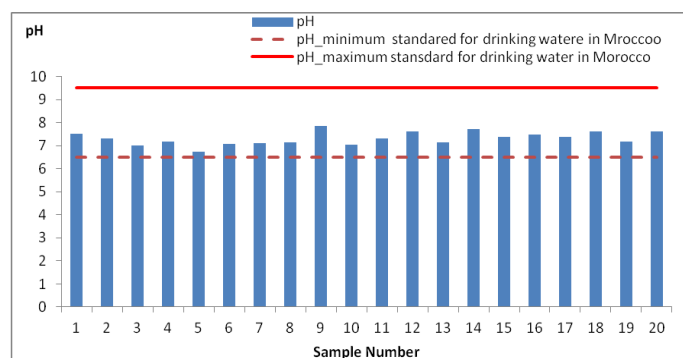


Fig. 2: Variation of pH in all samples

Electrical Conductivity (EC)

EC means the ability of a solution to conduct electrical conductivity. This notion is inversely proportional to that of electrical resistivity and depends on several factors such as the presence of ions and their concentrations (Rodier *et al.*, 2009). The EC recorded in the waters varies between 1540 to 17550 $\mu\text{s}/\text{cm}$ with an average value of 4915 ± 3772 (Table 1). According to the Moroccan drinking Water standard, 25% of the tested samples are of average qualified where about 75 % of the samples are unqualified. (Fig. 3).

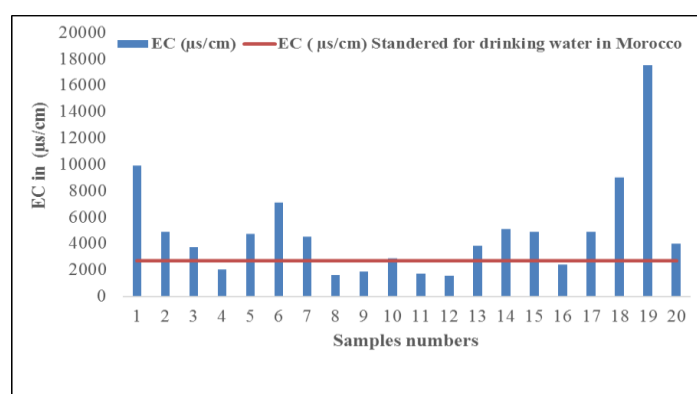


Fig. 3: Variation of Electrical Conductivity of the samples

Cation chemistry (Ca^{2+} , Mg^{2+} , Na^+ , K^+)

Calcium (Ca^{2+})

Calcium (Ca^{2+}) is present in the crystalline rocks and sedimentary rocks. It is very soluble and widely presented in most water (MacGregor, 2012). The concentration of Calcium was found in the range between 56.8 and 290 mg/L with an average 167.46 ± 70.5 (Table 1). According to Moroccan standards for drinking water, 35% of the collected well water is qualified, and 65 % of the well water are above the standard levels (Fig.4a).

Magnesium (Mg^{2+})

The concentration of Magnesium was found in the range of 26.64-192.2 mg/L with an average 71.12 ± 42.58 (Table 1). These results are consistent with the Moroccan standards. The quality of collected water according to Mg^{2+} concentration can be divided to 35% is excellent quality, 45% are good quality and 15% is bad quality (Fig. 4b).

Sodium (Na^+)

The sodium (Na^+) is very abundant on earth. It is found in the crystalline rocks and sedimentary rocks sands and clays. The rock Halite (NaCl) is a salt (Ahmad and Ahmad, 2003). Na^+ is very soluble in water. The concentration of Na^+ was ranged

between 186-1959 mg/l with an average 738.04 ± 507 (Table 1). According to the Moroccan standards for drinking water, only 5% of the samples are in excellent quality water, and 95% are in bad quality (Fig. 4c).

Potassium (K^+)

The main sources of potassium are crystalline rocks, clays and fertilizers (Appelo and Postma, 2004; MacGregor, 2012). The concentration of (K^+) was found in the range between 2.34 -11.7 with an average 5.946 ± 2.742 , It is acceptable according to Moroccan standards, (Table 1 and Fig. 4d).

Anion chemistry (HCO_3^- , Cl^- , SO_4^{2-} , NO_3^-)

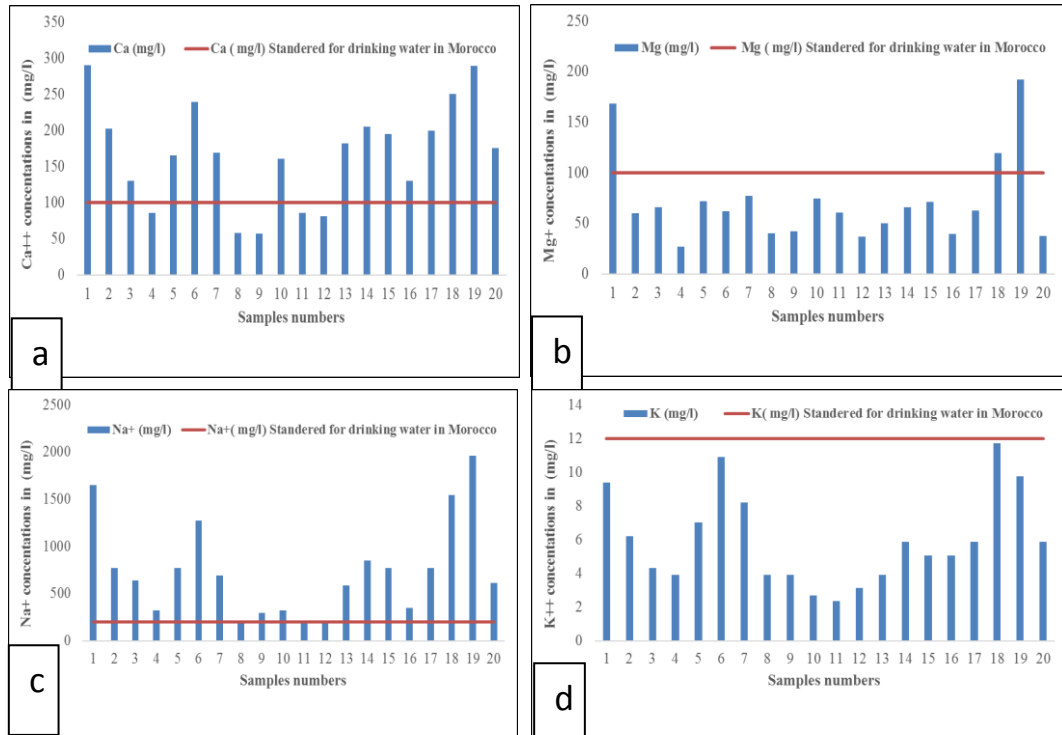


Fig. 4: Variation of Cation chemistry (Ca^{2+} , Mg^{2+} , Na^+ , K^+)

Chloride (Cl^-)

Chloride (Cl^-) is present naturally in groundwater due to leaching of sedimentary rocks and soils, as well as the dissolution of salt deposits (Logeshkumaran *et al.*, 2015). The concentration of Cl^- in the tested water samples was found in the range of (264.83- 2928.75 mg/l) with an average (1111.37 ± 776) (Table 1). According to Moroccan standards for drinking water, 35% of the samples are in acceptable quality where 65% are not (Fig. 5a).

Sulfates (SO_4^{2-})

The Sulfates (SO_4^{2-}) can be found in all natural waters. The origin of the sulfate compounds is oxidation of theores of sulfates. Sulfate is one of the major compounds that dissolved in rainwater (Appelo and Postma, 2004). The concentration of SO_4^{2-} was found in the range of (13.7 and 223.4 mg/l) with an average value (79 ± 58) (Table 1). According to the Moroccan standard, all samples were within the acceptable range for drinking standards (Fig 5b).

Bicarbonate (HCO_3^-)

The concentrations of HCO_3^- in the samples were found in the range of 145.2 - 799.1 mg/L with mean value of 134.22 mg/L, (Table 1 and Fig. 5c). Most samples were in the acceptable range according to the Moroccan standard.

Nitrate (NO_3^-)

The concentration of nitrates in groundwater and surface water is low, but it can reach high levels due to leaching of cultivated land or contamination by the waste of human or animal origin WHO, (2003). The concentrations of NO_3^- in the samples were in the range of 14.26–386.88 mg/l with an average 99.5 (Table 1 & Fig. 5d). It was observed that the highest concentrations are recorded in areas with agricultural activities.

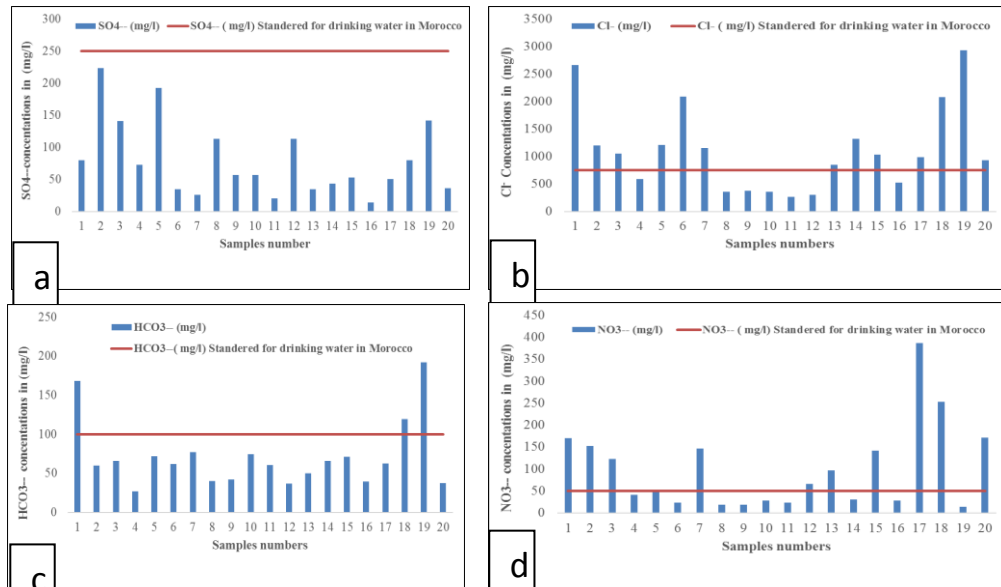


Fig. 5. variation of Anion chemistry (Chloride, Sulfate, Nitrates and bicarbonate) of all samples.

Ammonium (NH_4^+)

Ammonia is a gas soluble in water; groundwater is usually low in ammonia nitrogen. The presence of ammonium in relatively large quantities can be an indication of pollution by releases of man-made or industrial (chemical industries, nitrogen fertilizer, coking plants, ice factory, textile) WHO (2011). The concentration of ammonium in the water samples was found in the range of 0.9 and 7.02 mg/l with an average 2.125 ± 1.302 (Table 1 & Fig. 6). According to Moroccan standard, all collected samples are unqualified as drinking water.

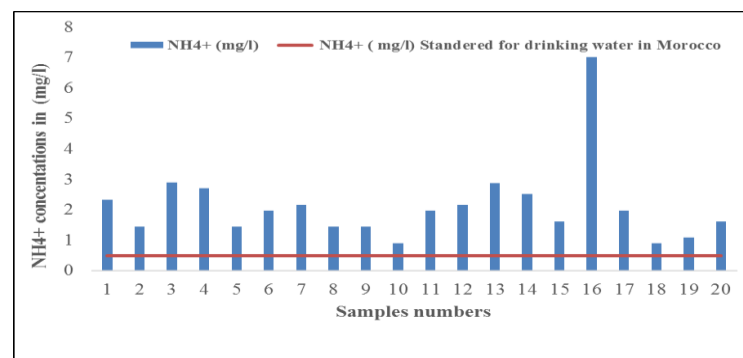


Fig. 6: Variation of Ammonium of all samples

Chemical Classification of Groundwater

Correlation matrix:

Correlation criterion between two variables is the simple correlation coefficient that indicates the sufficiency of one variable to predict the other (Benesty *et al.*, 2009).

(Table 2), showed the values of the correlation coefficients of the elements. The correlation matrix of 11 physicochemical parameters of the study area were presented as follows: Strong correlation is ($r > 0.9$) and a good correlation is between ($r = 0.5$ to 0.9).

Table 2: Correlation matrix of 11 physicochemical parameters

Variables	EC μs/cm	pH	Ca ²⁺	Mg ²⁺	Na ⁺	K ⁺	Cl ⁻	SO ₄ ²⁻	HCO ₃ ⁻	NO ₃ ⁻	NH ₄ ⁺
EC μs/cm	1.00	-0.07	0.85	0.91	0.95	0.77	0.93	0.23	0.63	0.14	-0.27
pH	-0.07	1.00	-0.06	-0.06	-0.02	-0.04	-0.07	-0.33	0.10	0.17	0.09
Ca ²⁺	0.85	-0.06	1.00	0.77	0.92	0.80	0.90	0.08	0.72	0.38	-0.19
Mg ²⁺	0.91	-0.06	0.77	1.00	0.88	0.66	0.86	0.21	0.66	0.14	-0.29
Na ⁺	0.95	-0.02	0.92	0.88	1.00	0.89	0.99	0.19	0.65	0.27	-0.26
K ⁺	0.77	-0.04	0.80	0.66	0.89	1.00	0.89	0.10	0.56	0.30	-0.18
Cl ⁻	0.93	-0.07	0.90	0.86	0.99	0.89	1.00	0.21	0.57	0.21	-0.22
SO ₄ ²⁻	0.23	-0.33	0.08	0.21	0.19	0.10	0.21	1.00	0.12	-0.01	-0.34
HCO ₃ ⁻	0.63	0.10	0.72	0.66	0.65	0.56	0.57	0.12	1.00	0.56	-0.19
NO ₃ ⁻	0.14	0.17	0.38	0.14	0.27	0.30	0.21	-0.01	0.56	1.00	-0.15
NH ₄ ⁺	-0.27	0.09	-0.19	-0.29	-0.26	-0.18	-0.22	-0.34	-0.19	-0.15	1.00

EC have strong correlations with Mg²⁺, Na⁺ and Cl⁻. Also strong correlations were found between Ca²⁺ and Cl⁻ as well between Na⁺ with Cl⁻

The correlations found for EC with Ca²⁺ and K⁺, also between Ca²⁺ with Mg²⁺, Na⁺ and K⁺, as well between Mg²⁺ with Na⁺, K⁺ and Cl⁻ in addition to Na⁺ with K⁺ also K⁺ with Cl⁻. Other Correlations parameters are bad correlations.

The piper Trilinear diagram

The Sidi Sileman groundwater samples are plotted in Piper Diagram (Fig. 7). The Figure shows the different groups of samples that have been summarized in (Table 3).

Table 3: Classification of groundwater samples based on the Piper trilinear diagram

Class	Groundwater types/characteristics of corresponding subdivisions of diamond shaped fields	Samples in the category	
		No. of samples	%
I	Ca ²⁺ -Mg ²⁺ -Cl ⁻ -SO ₄ ²⁻	2	10
II	Na ⁺ - K ⁺ - Cl ⁻ -SO ₄ ²⁻	18	90
III	Na ⁺ - K ⁺ - HCO ₃ ⁻	0	0
IV	Ca ²⁺ -Mg ²⁺ - HCO ₃ ⁻	0	0
1, 4, 5	Alkaline earth (Ca + Mg) exceed alkalies (Na + K)	2	10
2, 3, 6	Alkalies exceeds alkaline earths	18	90
3,1,6	Weak acids (CO ₃ + HCO ₃) exceed strong acids (SO ₄ +Cl)	0	0
4,2,5	Strong acids exceeds weak acids	20	100
1	HCO ₃ -CO ₃ and Ca-Mg (temporary hardness); magnesium bicarbonate type (carbonate hardness exceeds 50 %)	0	0
5	SO ₄ -Cl and Ca-Mg (permanent hardness); calcium chloride type (non-carbonate hardness exceeds 50 %)	0	0
2	SO-Cl and Na-K (saline); sodium chloride type (non-carbonate alkali exceeds 50 %)	18	90
6	HCO ₃ -CO ₃ and Na-K (alkali carbonate); sodium bicarbonate type (carbonate alkali exceeds 50 %)	0	0
3, 4	Mixing zone (no one cation-anion exceed 50 %)	2	10

The results showed that out of 20 samples, 90% of the samples belong to (Na⁺-K⁺- Cl⁻-SO₄²⁻) type and only 10 % samples fall under (Ca²⁺-Mg²⁺-Cl⁻-SO₄²⁻) type, (Fig. 7) also illustrating the absence of both permanent and temporary hardness (class1 and 5) in the groundwater of the Sidi Slimane regain. It is also observed from

(Fig. 7) That most of the groundwater samples (90 %) are in zone 2, SO–Cl and Na–K; where types of groundwater identified as sodium chloride type dominant. Hence water types originating from halite dissolution (saline). While those falling under zone 4 (10 %) belong to the mixed zone, where types of groundwater cannot be identified as neither anion nor cation dominant (Todd and Mays, 2005). It is evident from piper plot, the graphs demonstrate the dominance of alkali over alkaline earths (i.e., $Ca + Mg > Na + K$), and strong acidic anions exceed weak acidic anions (i.e., $Cl + SO_4 > HCO_3$) as in class 4,2,5 in table 3. None of the samples fall under zone 6 or 5 giving an indication of weak enrichment of the alkali carbonate and non-carbonate hardness exceeds 50 %, (type originating from limestone and dolomite are absence).

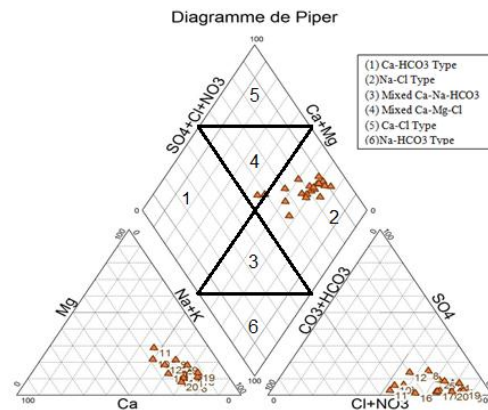


Fig. 7: piper diagram of all samples.

The piper diagram was preferred to other conventional methods because it allows a more precise identification for the samples and some dominant processed in the water chemistry (Overstreet *et al.*, 1985). The Piper trilinear diagram can be used to illustrate the similarities and differences in the composition of waters and to classify them into certain chemical types (Piper, 1944). The geology of the Sidi Slimane area is generally sedimentary rock composition which has affected the groundwater quality.

Principal Component Analysis (PCA)

PCA is a powerful technique for pattern recognition that attempts to explain the variance of a large set of intercorrelated variables. It indicates association between variables, thus, reducing the dimensionality of the dataset. PCA extracts the eigenvalues and eigenvectors from the covariance matrix of original variables. The principal components (PCs) are the uncorrelated (orthogonal) variables, obtained by multiplying the original correlated variables with the eigenvector (loadings). The eigen values of the PCs are the measure of their associated variance, the participation of the original variables in the PCs is given by the loadings, and the individual transformed observations are called scores (Ravikumar and Somashekar, 2017). PCA of data was used to reduce the number of mathematical components or factors which can be used to provide a basis for the data set and to detect the presence of any sample groups, patterns, similarities and differences which can be described in score plots (Al Maliki *et al.*, 2014). The Factors are in linear combinations of the starting variables. Each variable contributing to the factor intervenes with a coefficient called "eigenvector" (Morell *et al.*, 1996; Sabnavis and Patangay, 1998; Bouderbala *et al.*, 2016). The PCA carried out on a data matrix consisting of 20 points representing prospected samples, and 11 columns representing physicochemical variables measured or analyzed following the criteria of Cattell and Jaspers (Benhamiche *et al.*, 2016), PCs

with eigenvalues >1 were retained. Table 4 summarizes the PCA results, including the loadings, eigenvalues and variance elucidated by each principal component (PCs). PCA rendered two PCs with eigenvalues >1 explaining 69.11% of the total variance of the dataset. As a result, the total variance of PCA were obtained by first two PC hardly exceed 69.11%. The loading and the score plots of the first two PCA are represented in Figs. (8 and 9) respectively. The score plot shown in (Fig. 8) represented the way of identifying a number of useful factors, The slope of the plot changes from high to low after the first two factors could be observed. The eigenvalues also drop below 1, suggests that a two component solution could be the right choice which includes the total variance of 69.11 %.

Table 4: Loadings of experimental variables on principal components, eigen values and variances for groundwater dataset

	F1	F2
EC $\mu\text{s}/\text{cm}$	0.384	-0.081
pH	-0.021	0.581
Ca^{2+}	0.378	0.097
Mg^{2+}	0.364	-0.078
Na^+	0.400	0.000
K^+	0.354	0.058
Cl^-	0.390	-0.041
SO_4^{2-}	0.095	-0.573
HCO_3^-	0.306	0.227
NO_3^-	0.145	0.390
NH_4^+	-0.128	0.321
Eigenvalue	6.059	1.543
Variability (%)	55.083	14.027
Cumulative %	55.083	69.110

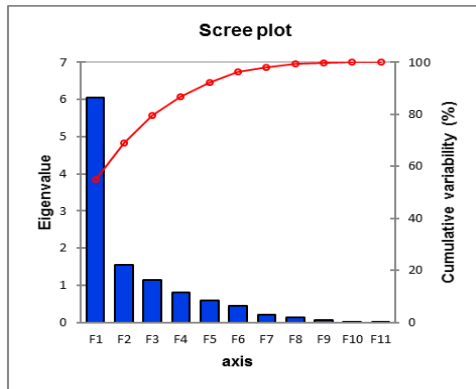


Fig. 8: Scree plot of all the variables.

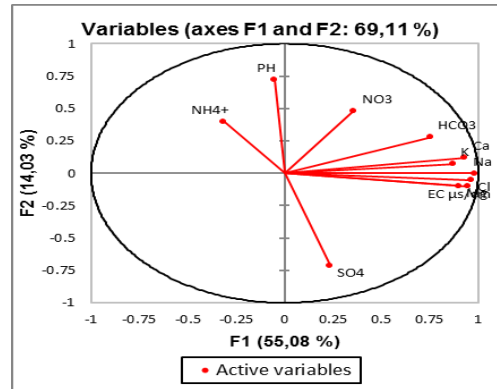


Fig. 9: PCs score plot for datasets of water samples

The loadings plot (Fig. 9) of the first two PCs (PC1 and PC2) shows the distribution of all the physico-chemical parameters, for the water samples from Sidi Slimane region. The scores plot showed mixed distribution of samples. Visible grouping of majority of the samples has been observed in the upper right and lower right quadrants while, loading of the rest samples are found to be noticeably scattered.

Grouping of parameters (EC , Ca^{2+} , Mg^{2+} , K^+ , Na^+ , HCO_3^- and Cl^-) and (pH , NH_4^+ , SO_4^{2-} and NO_3^-) in the loadings plot suggests their significant mutual positive correlation. The PCs score plots portray the characteristics of the samples and aid to comprehend their spatial distribution.

The plots of PCA loadings scores for dataset of groundwater samples (Fig. 10) showed the clustering of site specific samples for dataset of water samples in space

and their spatial distribution, from this figure, it is possible to understand the relations between the measured elements, as follows:

The first PC mainly describes samples with a higher concentration of (EC), (Ca^{2+}), (Mg^{2+}), (HCO_3^-), (SO_4^{2-}), (Na^+), (K^+) and (Cl^-). In the corresponding score plot, the first PC includes wells no. (19, 6, 1, 7, 17, 2, 5 and 15), these samples were characterized by high conductivity and some metal ion concentrations. The output of this plot is in confirmation with correlation matrix (Table 2). The second PC illustrates samples with high pH, Sulfate, Nitrate, and Ammonium and include samples no. (3, 10, 11, 12, 9, 8, 14, 18, 20, 13, 4 and 16).

The PCs scores plot (Fig. 9) Constructed using PC1 and PC2 components confirms the clustering of site specific samples in space and their spatial distribution (Fig. 10).

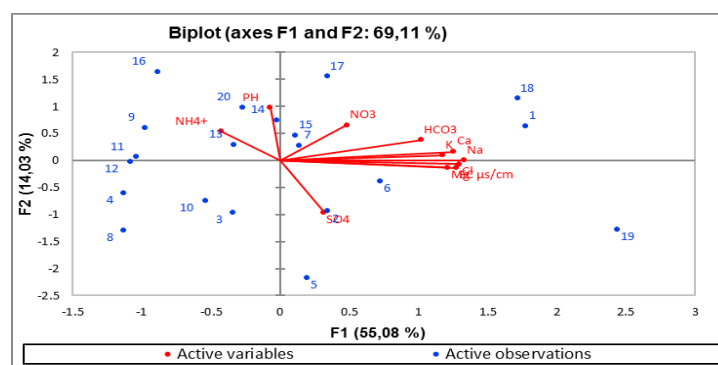


Fig. 10: Plots of PCA loadings scores for dataset of groundwater samples.

CONCLUSION

It is very important to determine the source of contamination in order to protect the groundwater. The present study demonstrated the importance of constructing graphical representations, such as Piper trilinear diagram plot using dissolved constituents (major cations and major anions) to effectively understand hydrochemical evolution, grouping and areal distribution of water facies of groundwater resources at Sidi Slimane area in Morocco. The piper plot classified 90 % of the samples under ($\text{Na}^+ - \text{K}^+ - \text{Cl}^- - \text{SO}_4^{2-}$) type where types of groundwater identified as sodium chloride type dominant, while those falling under ($\text{Ca}^{2+} - \text{Mg}^{2+} - \text{Cl}^- - \text{SO}_4^{2-}$) type belong to the mixed zone with no one cation–anion pair exceeding 50 % in the majority of the analyzed samples. It is therefore evident that primary salinity and secondary alkalinity were dominant in the majority of samples as indicated by permanent (non-carbonate) hardness. The piper plots further confirmed the existence of alkali over alkaline earths (i.e., $\text{Ca}^{2+} + \text{Mg}^{2+} > \text{Na}^+ + \text{K}^+$), and strong acidic anions exceed weak acidic anions (i.e., $\text{Cl}^- + \text{SO}_4^{2-} > \text{HCO}_3^-$). Based on the criteria specified in Moroccan standards for drinking water quality, the collected groundwater samples are considered unsuitable for drinking, which refers to the geological structure of the area studied. The plots of PCA loadings scores for a dataset of groundwater samples demonstrated the clustering of site-specific samples for the dataset of groundwater samples in space and their spatial distribution, which is relieving to understand the relations between the measured elements, the output of this plot is in confirmation with correlation matrix and Piper diagram results. The present work recommends using the Piper trilinear diagram technique widely, to evaluate the quality of groundwater and understand the hydrochemical facies characteristics.

ACKNOWLEDGMENT

The Authors are thankful to The National Key Research and Development Program (2017YFB0503900), Science and technology cooperation project of Sanya municipal institute (2018YD10) and National Science and Technology (05-Y30B01-9001-19/20-1) for supporting this research. The authors are also thankful to Laboratory of Agro-physiology, Biotechnology, Environment and Quality, Faculty of Sciences, Ibn Tofail University, Kenitra, BP.133, Morocco for offering the fund for the laboratory analysis.

REFERENCES

- Abd El Aal, S.; Abdelhady, A.; Mansour, N.; Hassan, N. M.; Elbaz, F. and Elmaghraby, E. K. (2019). Physical and chemical characteristics of hematite nanoparticles prepared using microwave-assisted synthesis and its application as adsorbent for Cu, Ni, Co, Cd and Pb from aqueous solution. *Materials Chemistry and Physics*, 121771. Doi:10.1016/j.matchemphys.2019.121771.
- Abdul-Kader, A. M.; Zaki, B, M. F.; El-Badry, A. (2014). Modified the optical and electrical properties of CR-39 by gamma ray irradiation. *J. Radiat. Res. Appl. Sci.*, 7(3): 286-291. Doi:10.1016/j.jrras.2014.05.002.
- Badawy, Z. M.; Zaki, M. F. and Elmaghraby, E. K. (2018). Investigations on the Migration of Radiation-Induced Compounds in Polymeric Nuclear Track Detectors. *Arab J. Nucl. Sci. Appl.*, 51 (3): 1-8. Doi:10.21608/ajnsa.2017.1868.1002.
- Baglin, C. M. (2002). Nuclear data sheets for A = 59. *Nucl. Data. Sheets*, 95(2): 215-386. Doi:10.1006/ndsh.2002.0004.
- Basunia, M. S. (2018). Nuclear Data sheets for A=59. *Nucl. Data Sheets*, 151, 1 – 333. Doi:10.1016/j.nds.2018.08.001.
- Bo Liu, Pu-Cheng Wang, Yin-Yong Ao, Yan Zhao, You An, Hong-Bing Chen and Wei Huang (2017). Effects of combined neutron and gamma irradiation upon silicone foam. *Radiat. Phys. Chem.*, 133, 31–36. Doi:10.1016/j.radphyschem.2016.12.005.
- Browne, E and Tuli, J. K. (2007). Nuclear data sheets for A = 137. *Nucl. Data Sheets*, 111(10): 2173 – 2318. Doi:10.1016/j.nds.2007.09.002.
- Browne, E. and Tuli, J., K. (2013). Nuclear data sheets for A = 60. *Nucl. Data. Sheets*, 114(12): 1849 – 2022. Doi:10.1016/j.nds.2013.11.002.
- Castillo, F.; Espinosa, G.; Golzarri, J. I.; Osorio, D.; Rangel, J.; Reyes, P.G. and Herrera, J.J.E. (2013). Fast neutron dosimetry using CR-39 track detectors with polyethylene as radiator. *Radiat. Meas.*, 50: 71-73. Doi: 10.1016/j.radmeas.2012.09.007.
- Claudia, R.; Benitez-Nelson; Sabine Charmasson; Ken Buesseler; Minhan Dai; Michio Aoyama; Núria Casacuberta; José Marcus Godoy; Andy Johnson; Vladimir Maderich; Pere Masqué; Marc Metian; Willard Moore; Paul, J.; Morris and John, N. Smith (2018). Radioactivity in the Marine Environment: Understanding the Basics of Radioecology. *Limnology and Oceanography e-Lectures*, 8: 170– 228. Doi:10.1002/loe2.10007.
- Clough, R. L. and Shalaby S. W. (1996). Irradiation of Polymers: Fundamentals and technological applications. American Chemical Society., Washington, DC.
- Dong, Y. and Junde, H. (2014). Nuclear data sheets for A = 54. *Nucl. Data. Sheets*, 121: 1 – 142. Doi:10.1016/j.nds.2014.09.001.

- El-Badry, B. A.; Zaki, M. F.; Abdul-Kader, A. M.; Tarek, M.; Hegazy, A.; Morsy, A. (2009). Ion bombardment of Poly-Allyl-Diglycol-Carbonate (CR-39). *Vacuum*, 83: 1138–1142. Doi:10.1016/j.vacuum.2009.02.010.
- Elmaghraby, E. K. and Seddik, U. (2015). Thermophysical properties and reaction kinetics of irradiated poly allyl diglycol carbonates nuclear track detector. *Radiat. Eff. Defects. Solids*, 170, 621–629. Doi:10.1080/10420150.2015.107733.
- Elmaghraby, E. K.; Saad Abdelaal; Abdelhady, A. M.; Samar Fares, Salama, S. and Mansour, N.A. (2020). Experimental determination of the fission-neutron fluence-to-dose conversion factor. *Nuclear Inst. and Methods in Physics Research, A.*, 949, 162889. Doi: 10.1016/j.nima.2019.162889.
- Elmaghraby, E. K. (2017). Resonant neutron-induced atomic displacements. *Nucl. Instrum. Methods Phys. Res. B*, 398, 42 – 47. Doi:10.1016/j.nimb.2017.03.054.
- Elmaghraby, E. K. and Talat, S. A. (2010). Investigation of the fluorescence emitted from polyallyl diglycol carbonate modified by gamma-ray radiation excited by UV radiation. *Radiat. Eff. Def. Solids.*, 165, 4, 321–328. Doi: 10.1080/10420150903452252.
- El-Saftawy, A. A.; Abdel Reheem, A. M.; Kandil, S. A.; Abd El Aal, S. A. and Salama, S. (2016). Comparative studies on PADC polymeric detector treated by gamma radiation and Ar ion beam. *Applied Surface Science*, 371: 596-606. Doi:10.1016/j.apsusc.2016.03.044.
- El-Saftawy, A. A.; Elfalaky, A.; Ragheb, M. S. and Zakhary, S. G. (2014). Electron beam induced surface modifications of PET film. *Radiat. Phys. Chem.*, 102: 96-102. Doi:10.1016/j.radphyschem.2014.04.025.
- El-Saftawy, A. A.; Abd El Aal, S. A.; Hassan, N. M. and Abdelrahman, M. M. (2016). Optical and chemical behaviors of CR-39 and Makrofol plastics under low-energy electron beam irradiation. *Japanese Journal of Applied Physics*, 55, 076401. Doi: 10.7567/jjap.55.076401.
- El-Said, H.; Ramadan, H. E.; Elmaghraby, E. K. and Amin, M. (2018). Development of granular radioactive reference source from $^{152,154}\text{Eu}$ adsorbed on tin tungstate matrix. *Radiochimica Acta*, 106, 8. [Doi: 10.1515/ract-2017-2885](https://doi.org/10.1515/ract-2017-2885).
- Firestone, R. B. and Revay, Z. (2016). Thermal neutron capture cross sections for $^{16,17,18}\text{O}$ and ^2H . *Phys. Rev. C.*, 93, 044311. Doi:10.1103/PhysRevC.93.044311.
- Hassan, A.; El-Saftawy, A. A.; Abd El Aal, S. A. and El Ghazaly, M. (2015). Irradiation influence on Mylar and Makrofol induced by argon ions in a plasma immersion ion implantation system. *Appl. Surf. Sci.*, 347: 784-792. Doi: 10.1016/j.apsusc.2015.04.179.
- Khazov, Y.; Rodionov, A. and Kondev, F. (2011). Nuclear data sheets for A = 133. *Nucl. Data Sheets*, 112(4): 855 – 1113. Doi:10.1016/j.nds.2011.03.001.
- Kulwinder Singh Mann; Asha Rani and Manmohan Singh Heer (2015). Shielding behaviors of some polymer and plastic material for gamma-rays, *Radiat. Phys. Chem.*, 106, 247–254. Doi: 10.1016/j.radphyschem.2014.08.005.
- Kumar, R. and Singh, P. (2013). UV–visible and infrared spectroscopic studies of Li^{3+} and C^{5+} irradiated PADC polymer. *Results in Physics*, 3: 122-128. Doi:10.1016/j.rinp.2013.07.001.
- Malek, M. A. and Chong, C. S. (2002). Generation of CO_2 in γ -ray irradiated CR-39 plastic, *Radiat. Meas.*, 35: 109-112. Doi: 10.1016/s1350-4487(01)00275-x.
- Martin, M., J. (2013). Nuclear data sheets for A = 152. *Nucl. Data. Sheets*, 114(11): 1497-1847. Doi:10.1016/j.nds.2013.11.001.
- Mee, L. D. and Readman, J. W. (1993). "Nuclear and isotopic techniques for investigating marine pollution." *IAEA Bulletin* 35 (2): 2-8.

- Mori, Y.; Yamauchi, T.; Kanasaki, M.; Hattori, A.; Oda, K.; Kodaira, S.; Konishi, T.; Yasuda, N.; Tojo, S.; Honda, Y. and Barillon, R. (2013). Vacuum effects on the radiation chemical yields in PADC films exposed to gamma rays and heavy ions. *Radiat. Meas.*, 50: 97 – 102. Doi:[10.1016/j.radmeas.2012.07.013](https://doi.org/10.1016/j.radmeas.2012.07.013)
- Nouh, S.A.; Amer, H. and Remon, S.W. (2009). Effect of neutron dose on the structural properties of Makrofol polycarbonate. *Nuclear Instruments and Methods in Physics Research*, 267: 1129–1134. Doi:10.1016/j.nimb.2009.02.049.
- Patrick landais (1995). Statistical determination of geochemical parameters of coal and kerogen macerals from transmission micro-infrared spectroscopy data. *Org. Geochem.*, 23 711-720. Doi: 10.1016/0146-6380(95)00070-U.
- Prävãlie, R. (2014). Nuclear Weapons Tests and Environmental Consequences: A Global Perspective *AMBIO*, 43, 729. Doi: 101007/s13280-014-0491-1.
- Rivaton, A. and Arnold, J. (2008). Structural modifications of polymers under the impact of fast neutrons. *Polymer Degradation and Stability*, 93(10): 1864-1868. Doi:10.1016/j.polymdegradstab.2008.07.015.
- Saad, A. F.; Hamed, N. A.; Abdalla, Y. K. and Tawati, D. M. (2012). Modifications of the registration properties of charged particles in a CR-39 polymeric track detector induced by thermal annealing. *Nuclear Instruments and Methods in Physics Research B*, 287, 60–67. Doi:10.1016/j.nimb.2012.07.005.
- Saad, A.F.; Mona, H.; Ibraheim, A.; Nwara, M. and Kandil, S.A. (2018). Modifications in the optical and thermal properties of a CR-39 polymeric detector induced by high doses of γ -radiation. *J.Radiat. Phys. Chem*, 145: 122–129. Doi:10.1016/j.radphyschem.2017.10.011.
- Sahoo, G.S.; Paul, S.; Tripathy, S. P.; Sharma, S. C.; Jena, S.; Rout, S.; Joshi, D.S. and Bandyopadhyay, T. (2014). Effects of neutron irradiation on optical and chemical properties of CR-39: Potential application in neutron dosimetry. *J. Appl. Radiat. Isot.*, 94: 200-205. Doi:10.1016/j.apradiso.2014.08.012.
- Sahoo, G.S.; Tripathy, S. P.; Paul, S.; Sharma, S. C.; Joshi, D. S.; Gupta, A. K. and Bandyopadhyay, T. (2015). Effects of high neutron doses and duration of the chemical etching on the optical properties of CR-39. *J. Appl. Radiat. Isot.*, 101: 114-121. Doi:10.1016/j.apradiso.2015.04.002.
- Sangeeta Prasher; Mukesh Kumar and Surinder Singh (2015). The influence of neutron irradiation in CR-39 polymer. *Oriental Journal of Chemistry*, 31(2): 1201-1204. Doi:10.13005/ojc/310277.
- Shaat, M. (2010). Utilization of ETRR-2 and collaboration. Report IAEA-TM-38728, IAEA, Austria.
- Siddhartha, Suveda Aarya; Kapil Dev; Mohd Shakir; Bashir Ahmed and Wahab, M. A. (2012). Effect of cobalt-60 γ radiation on the physical and chemical properties of poly (ethylene terephthalate) polymer. *J. Appl. Polym. Sci.*, 125: 3575–3581. Doi:10.1002/app.36397.
- Srivastava, A.; Singh, T. V.; Mule, S.; Rajan, C. R. and Ponrathnam, S. (2002). Study of chemical, optical and thermal modifications induced by 100 MeV silicon ions in a polycarbonate film. *Nucl. Instrum. Methods. Phys. Res. Sect B.*, 192: 402–6. Doi: 10.1016/S0168-583X(02)00493-7.
- Talat, A. S. and Elmaghraby, E. K. (2010). High gamma-ray dose measurement using nuclear track detector. *J. Radiat. Protect. Dosim.*, 140 (3): 218–222. Doi: 10.1080/10420150903452252.
- Yamauchi, T.; Nakai, H.; Somaki, Y. and Oda, K. (2003). Formation of CO₂ gas and OH groups in CR-39 plastics due to gamma-ray and ions irradiation, *Radiat. Meas.* 36: 99-103. Doi: 10.1016/s1350-4487(03)00102-1.

- Zaki, M. F.; Elmaghraby, E. K. and Elbasaty, A. B. (2016). Structural alterations of polycarbonate/PBT by gamma irradiation for high technology applications. *Journal of Adhesion Science and Technology* 30(4): 443–457. Doi:10.1080/01694243.2015.1105123.
- Zaki, M. F. and Elmaghraby E. K. (2008). Photoluminescence of irradiation induced defects on CR-39. *Philosophical Magazine*. 88, 23, 11: 2945–2951. Doi: 10.1080/14786430802447052.
- Zhou, D.; Semones, E.; Mark, D. Weyland and Benton, E. R. (2007). LET calibration for CR-39 detectors in different oxygen environments. *Radiat. Meas.*, 42(9): 1499–1506.